

RESEARCH
PAPER



Has the advancing onset of spring vegetation green-up slowed down or changed abruptly over the last three decades?

Xuhui Wang^{1,2}, Shilong Piao^{1,3*}, Xiangtao Xu¹, Philippe Ciais⁴,
Natasha MacBean⁴, Ranga B. Myneni⁵ and Laurent Li²

¹College of Urban and Environmental Sciences, Peking University, Beijing 100871, China,

²Laboratoire de Météorologie Dynamique, IPSL, CNRS/UPMC, Paris 75005, France, ³Key Laboratory of Alpine Ecology and Biodiversity, Institute of Tibetan Plateau Research, Center for Excellence in Tibetan Earth Science, CAS, Beijing 100085, China, ⁴Laboratoire des Sciences du Climat et de l'Environnement, CEA CNRS UVSQ, Gif-sur-Yvette 91191, France, ⁵Department of Earth and Environment, Boston University, 675 Commonwealth Avenue, Boston, MA 02215, USA

ABSTRACT

Aim Change in spring phenology is a sensitive indicator of ecosystem response to climate change, and exerts first-order control on the ecosystem carbon and hydrological cycles. The start of season (SOS) in spring can be estimated from satellite data using different spatiotemporal scales, data sets and algorithms. To address the impacts of these differences on trends of SOS, a Bayesian analysis is applied to investigate the rate of SOS advance and whether that advance has slowed down or changed abruptly over the last three decades.

Location 30°–75° N in the Northern Hemisphere.

Methods We applied four algorithms to three different satellite data sets (AVHRR, Terra-MODIS and SPOT) to obtain an ensemble of SOS estimates. A Bayesian analysis was applied to test different hypotheses of SOS trends.

Results Over the period 1982–2011, SOS is likely (74%) to have experienced a significant advance best described by a linear trend (-1.4 ± 0.6 days decade⁻¹). At hemispheric and continental scales, deceleration or abrupt changes in the SOS trend are unlikely (< 30%) to have occurred. Trend analysis restricted to the last decade suggests no significant SOS advance since 2000. This lack of trend can be explained by large interannual variations of SOS and uncertainties in SOS extraction, in the context of a short-term decadal-period analysis. Spatial analyses show that SOS advance could have slowed down over parts of western North America, and the SOS trend could have abruptly changed over parts of Canada and Siberia.

Main conclusions SOS advance is unlikely to have slowed down or changed abruptly at a hemispheric scale over the last three decades. At a regional scale, SOS advance could have slowed down or abruptly changed due to changes in winter chilling or fire regimes. Trends of SOS derived from different satellites were within the uncertainties of SOS extraction.

Keywords

Bayesian analysis, Northern Hemisphere, reversible-jump Markov-chain Monte-Carlo, satellite data, spring phenology, trend change.

*Correspondence: Shilong Piao, College of Urban and Environmental Sciences, Peking University, Beijing 100871, China.
E-mail: slpiao@pku.edu.cn

INTRODUCTION

Research interest into phenological changes has been increasing because phenology is a sensitive indicator of climate change (Menzel *et al.*, 2006) and has impacts on the terrestrial water and carbon cycles, with consequent feedbacks to climate

(Peñuelas *et al.*, 2009; Richardson *et al.*, 2013). Field data have traditionally been collected for individual plants, but they are limited in their spatial representation (Cleland *et al.*, 2007); On the other hand, long-term satellite imagery, such as NOAA-AVHRR data, provides land-surface phenology (LSP) estimates at an ecosystem level (Stöckli & Vidale, 2004). Despite the

difference in scale from individual plant phenology, LSP estimates enable studies to be carried out at regional or continental scales (Tucker *et al.*, 2001; Julien & Sobrino, 2009; Jeong *et al.*, 2011; Zeng *et al.*, 2011).

Normalized difference vegetation index (NDVI) data were first applied to the study of the start of the growing season in spring ('start of season', SOS) in the early 1970s (Henebry & de Beurs, 2013). Since then, a number of studies have used NDVI data to investigate changes in vegetation phenology across the Northern Hemisphere (NH) (Tucker *et al.*, 2001; White *et al.*, 2009; Jeong *et al.*, 2011; Zeng *et al.*, 2011). One major discovery was a significant and widespread advance of SOS over the NH during the 1980s and 1990s, although the magnitude of the trend varied between studies (Stöckli & Vidale, 2004; de Beurs & Henebry, 2005a; Julien & Sobrino, 2009; Jeong *et al.*, 2011). As longer time-series of data have become available, however, a few recent studies have suggested that the advancing trend of SOS has stalled or even reversed since the late 1990s in regions such as north-western North America or the Tibetan Plateau (Yu *et al.*, 2010; Jeong *et al.*, 2011; Piao *et al.*, 2011). For example, Jeong *et al.* (2011) reported that SOS advanced across the NH by 5.2 days from 1982 to 1999, but only by 0.2 days from 2000 to 2008. This potential slow-down of SOS needs to be carefully examined given its significant implications for climate–vegetation interactions.

One of the major uncertainties associated with satellite-derived phenology change lies in the different algorithms used for interpreting NDVI change in terms of vegetation phenophases. The choice of a particular algorithm strongly affects estimates of spatiotemporal changes in vegetation phenology (White *et al.*, 2009). For instance, one recent study showed that the trend of SOS in temperate China could vary by a factor of five depending on the algorithm used (Cong *et al.*, 2013). Despite recognition of these uncertainties in phenology detection (White *et al.*, 2009; Cong *et al.*, 2013), the effects of different algorithms on the diagnostic of trends in SOS have not been systematically studied. Thus, it is natural to question whether the recently observed shift in SOS trend is robust to the uncertainties induced by satellite phenology extraction algorithms.

The objectives of this study are thus (1) to investigate whether the SOS advance has slowed down or changed abruptly over the last three decades and (2) to investigate how algorithms of NDVI filtering in SOS extraction affect the statistics and regional patterns of SOS trends. To address these questions, we used four different algorithms to obtain SOS from satellite NDVI, and then applied a Bayesian approach to infer 30-year changes of SOS over 30°–75° N in the Northern Hemisphere.

MATERIALS AND METHODS

Data sets and preprocessing

We employed the third-generation NDVI data set (NDVI3g) derived from the AVHRR (Advanced Very High Resolution Radiometer) on-board NOAA (the National Oceanic and

Atmospheric Administration) satellites. The NDVI3g data set is currently available from 1982 to 2011 with images taken every two weeks at 5-arcminute spatial resolution. A series of corrections have been made in order to minimize the contamination introduced by aerosols, clouds and changes in solar zenith angle. The new generation of NDVI data includes corrections for potential discontinuities (step changes) due to sensor change. Previous studies have shown no step change in the entire course of the 30-year data (Pinzon & Tucker, 2014), and have successfully applied this data set to study the change in vegetation greenness and seasonality over the last three decades (e.g. Xu *et al.*, 2013).

Two additional NDVI data sets were also used: SPOT Vegetation (Satellite Pour l'Observation de la Terre vegetation sensor) and MODIS (Moderate Resolution Imaging Spectroradiometer). The SPOT NDVI data set is derived from the sensor on board the SPOT-4 and SPOT-5 satellites. Data are available at 10-day temporal resolution and a spatial resolution of *c.* 1 km from 1999. Atmospheric contaminations were corrected using the 'simple method for atmospheric correction' (SMAC) algorithm (Maisongrande *et al.*, 2004).

The MODIS NDVI data set (Collection 5 of MOD13A2) is derived from the MODIS sensor on board NASA's Terra satellite. Data are available at 16-day temporal resolution and 1-km spatial resolution from 2000. The product has minimized cloud contamination through the maximum-value composite procedure, and minimized the effects of anisotropy using the bidirectional reflectance distribution composite (BRDF; Huete *et al.*, 2002). To make the detection of phenology from SPOT and MODIS data comparable with AVHRR data, both NDVI data sets were resampled to 10-km resolution before the application of SOS extraction algorithms.

Daily freeze–thaw status of the ground was obtained from passive microwave satellites that observe dielectric changes that occur as the water in vegetation, surface snow and soil changes between predominantly frozen and thawed conditions (Kim *et al.*, 2012). The data set divides the landscape into frozen or non-frozen states as detected by microwave sensors on board a series of satellites (SMMR and SSM/I). The data set has global coverage from 1979 to 2010 with a spatial resolution of 25 km. It has been used in recent studies to determine the period available for vegetation growth (e.g. Xu *et al.*, 2013). A detailed description of the data set can be found in Kim *et al.* (2012).

The climate data set used in this study was the reanalysis product (ERA-Interim) from the European Centre for Medium-Range Weather Forecasts (ECMWF). The data set has subdaily temporal resolution available from 1979 to the present with a spatial resolution of 0.75° (Dee *et al.*, 2011). We defined pre-season temperature as the average daily temperature during the 90 days before the SOS for each pixel. We chose this period because the correlation between variations in SOS and pre-season temperature is strongest across 90% of the pixels when pre-season is defined as the period no more than 90 days before SOS (Jeong *et al.*, 2011; Cong *et al.*, 2013).

Management practices could exert a strong influence on land-surface phenology (LSP) dynamics. To minimize management

impacts, agricultural land and urban areas were excluded from our study. We further used a management intensity map (Luyssaert *et al.*, 2014) to exclude land areas with medium or intensive management practices. Evergreen forests were also excluded because of a lack of seasonality in NDVI time-series.

Extraction of SOS from NDVI time series

Four different algorithms – HANTS (harmonic analysis of time series), spline, polyfit and timesat – were applied to satellite NDVI data in order to obtain SOS estimates. The four algorithms used here represent various approaches used to filter potential data noise and reconstruct the seasonality in vegetation greenness. One or more of the algorithms have been used in recent studies of LSP (e.g. Julien & Sobrino, 2009; Jeong *et al.*, 2011; Barichivich *et al.*, 2013; Cong *et al.*, 2013). SOS is defined as the date at which the rate of increase of NDVI is highest. (See Supporting Information for the detailed scheme of the SOS extraction.)

Bayesian framework to determine SOS change

SOS trends are usually estimated by correlating or regressing SOS time-series against time, using the least-squares method (e.g. Jeong *et al.*, 2011; Cong *et al.*, 2013). The underlying assumptions of a linear regression, however, including normality and homogeneity of variance, may not always apply to SOS time-series, possibly resulting in spurious trends and biased statistical inferences (de Beurs & Henebry, 2005b). The alternative Markov chain Monte Carlo (MCMC) method is able to produce statistically unbiased estimates of trends under these conditions because it can simulate the posterior probability of model parameters when the observation errors do not follow a normal distribution or the time-series has non-constant variations.

Changes in trend are usually detected either by setting a fixed date (Jeong *et al.*, 2011), or by breakpoint-detection algorithms (e.g. de Jong *et al.*, 2012). These methods could suffer from temporally varying interannual variability in the time-series (Forkel *et al.*, 2013). The selection of trend models could also be addressed using information criteria, such as the Akaike information criterion or the Bayesian information criterion, but it remains challenging for these methods to simultaneously account for the uncertainties in the time-series data (see Supporting Information). In this study, we used a Bayesian algorithm (reversible-jump Markov chain Monte Carlo, RJ-MCMC)

to assess the probabilities of candidate models for SOS change, and to estimate their parameters (see details in Supporting Information).

Candidate models for SOS change

We included three models of SOS change: a linear model, a piecewise model and a shift model (Fig. 1). The linear model assumes a constant trend over the entire study period, whereas in the other two, change in trend is either continuous (piecewise model) or abrupt (shift model). These three models have 2, 4 and 5 parameters, respectively, and have been used to fit vegetation change in previous studies, but their results have rarely been compared (de Beurs & Henebry, 2004, 2005a,b; Jeong *et al.*, 2011; Wang *et al.*, 2011; de Jong *et al.*, 2012; Barichivich *et al.*, 2013). They are described by the following equations:

$$\text{Linear: } y_i = b_1 + b_2 t_i \quad (1)$$

$$\text{Piecewise: } y_i = \begin{cases} b_1 + b_2 t_i, & t_i < b_3 \\ b_1 + b_2 t_i + b_4 (t_i - b_3), & t_i \geq b_3 \end{cases} \quad (2)$$

$$\text{Shift: } y_i = \begin{cases} b_1 + b_2 t_i, & t_i < b_3 \\ b_5 + b_4 t_i, & t_i \geq b_3 \end{cases} \quad (3)$$

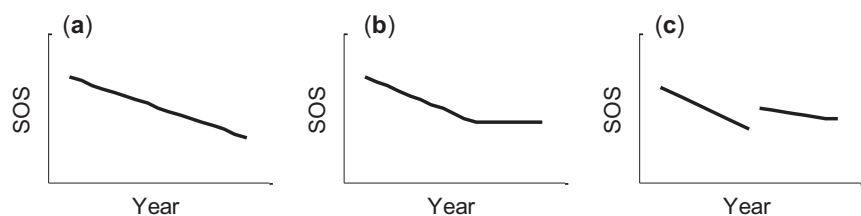
where b_1, b_2, \dots, b_5 are the fitted parameters, t_i is the year and y_i is the SOS value of that year. Although some parameters might share the same notation in three models (e.g. b_1 and b_2), their interpretations differ between models. A two-tailed t -test was applied to examine the statistical significance of the fitted parameters.

RESULTS

Spatial pattern of SOS

Mean SOS ranged from day 60 (early March) at lower latitudes to day 170 (late June) in the Arctic, around a median value of day 126 (see Fig. 2 for the spatial distribution of 30-year average SOS between 30° N and 75° N, estimated as the mean of the four algorithms applied to AVHRR NDVI data). SOS occurred earlier along the eastern coasts of the Atlantic and Pacific oceans than at the same latitudes along the western coasts. The Rocky Mountains, Scandinavian Mountains, Urals and the Tibetan Plateau experience SOS later than the surrounding lower-elevation areas (Fig. 2).

Figure 1 Diagrammatical summary of the three candidate models used for detecting changes in start of season (SOS) over the period 1982–2011: (a) linear model; (b) piecewise model ('piecewise'); and (c) model with an abrupt change ('shift').



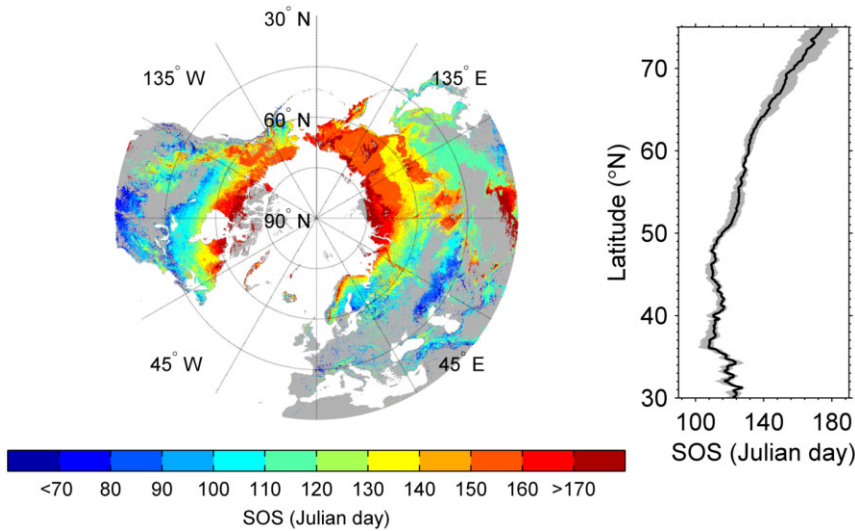


Figure 2 Spatial distribution of the 30-year average start of season (SOS) over 30°–75° N of the Northern Hemisphere (NH) estimated by the ensemble mean of the four SOS extraction algorithms. The black line in the right-hand panel shows the longitudinal average SOS estimated by the ensemble mean of each latitude. The inter-algorithm range of the longitudinal average SOS is shown in grey. The differences of 30-year average SOS estimated by four algorithms (see Methods section) are shown in Fig. S1.

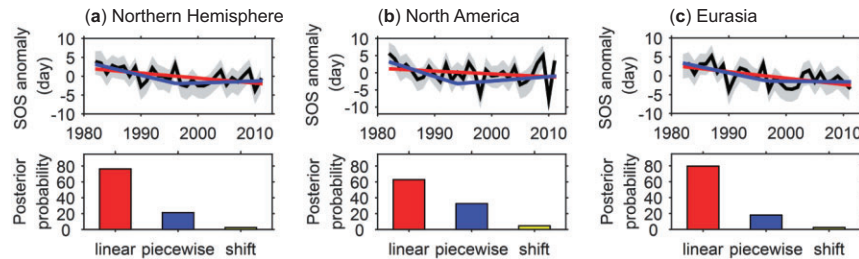


Figure 3 Change in start of season (SOS) over the period 1982–2011 across (a) the Northern Hemisphere (NH), (b) North America, and (c) Eurasia. In the upper panel, the black line and grey areas show the ensemble means and inter-model ranges of the SOS estimated by the four algorithms. Coloured lines show different model fit to change in SOS (red, linear model; blue, piecewise model; yellow, shift model) estimated by reversible-jump Markov chain Monte Carlo (RJ-MCMC). The lower panel shows the posterior probability of the three models under RJ-MCMC. Models with posterior probabilities below 0.1 are not shown in the upper panel. DOY, day of year.

Uncertainties due to different SOS extraction algorithms also varied spatially. The range (maximum–minimum) of average SOS dates from the four algorithms varied between 2 and 20 days at different latitudes (Fig. 2). South of 65° N, the inter-method range was less than 2 weeks, but it increased to 3 weeks in the Arctic. In the temperate zone, mean SOS values derived from polyfit, spline and timesat were all similar, but estimates from HANTS were systematically earlier than the other methods (Fig. S1). In the Arctic, however, SOS values from HANTS and timesat were similar, whereas those from polyfit and spline tended to occur later (Fig. S1).

SOS change at hemispheric and continental scales

To study temporal change in SOS, we first examined the area-weighted average SOS over the Northern Hemisphere between 30° N and 75° N ('NH' hereafter). There were positive anomalies during the 1980s and early 1990s and negative anomalies in 1990, 1998, 2000 and 2010 (Fig. 3a). The earliest SOS on record occurred in 2010. The inter-algorithm range of area-weighted SOS (grey area in Fig. 3a) was about 6–7 days, and varied slightly from year to year. Results from RJ-MCMC showed that SOS was

most likely to have experienced a linear advancing trend over the past 30 years (two-tailed *t*-test, $P < 0.01$), because the linear model had the highest posterior probability (74%) of the three candidate models. The trend was -1.4 ± 0.6 days per decade. The likelihood of SOS advance having stalled since the mid-1990s was 23% (Fig. 3a), and abrupt changes (at the scale of the huge region considered here) were extremely unlikely (< 3%).

Because previous studies have suggested that NDVI trends and variability differ between North America and Eurasia (Barichivich *et al.*, 2013), we also compared SOS changes between the two continents. For North America, the linear model was the most likely (62%) model to describe spatially averaged SOS change (Fig. 3b), but the rate of SOS advance (-0.8 ± 0.7 days per decade) was not significant ($P > 0.10$). We found a 34% probability that the change of SOS over North America was described by the piecewise linear model, with a period of advance (-4.6 ± 4.8 days per decade) before 1994 followed by a period of delay (1.6 ± 7.2 days per decade) after 1994 (Fig. 3b). By contrast, spatially averaged SOS significantly and consistently advanced over Eurasia with a trend of -1.7 ± 0.6 days per decade ($P < 0.01$) (Fig. 3c). A linear trend model was more likely to explain the data over Eurasia (79%) than over

North America (62%). For both continents, abrupt changes are extremely unlikely (< 4%; Fig. 3b,c).

SOS change at different latitudes

The SOS trends over North America varied latitudinally from -2.8 ± 0.7 days per decade in the south to 1.4 ± 1.8 days per decade in the north (Fig. 4a). Significant SOS advances were only found south of 50° N, and slight delays in SOS were seen north of 70° N. Results from RJ-MCMC showed that about 60% of the latitudinal bands over North America did not exhibit a high probability of trend change (Fig. S2a). One remarkable feature, however, was that for a band of latitudes between 45° N and 50° N, an abrupt SOS change had more than 50% probability of having occurred (Fig. S2a).

Across Eurasia, positive anomalies of SOS were concentrated at all latitudes in the 1980s and early 1990s, and negative ones in 1990, the late 1990s and the 2000s. All the latitudinal bands showed SOS advance with trends from -4.8 ± 0.8 to -0.1 ± 0.5 days per decade (Fig. 4b). We found that a stall in the SOS

advance could have occurred between 40° N and 55° N (probability > 50%), with SOS over this region occurring later during the late 2000s than the late 1990s (Fig. 4b).

Spatial patterns of SOS change

The linear model had the highest probability of the three candidate models over 55% of the study area (Fig. 5a–c). The regions that are most likely to have experienced linear advancement over the past three decades include the Arctic part of North America, western and northern Europe, southern areas of central Asia and the north-eastern part of East Asia. More than 80% of the pixels showed SOS advance (Fig. 5f), with the largest velocities (> 3 days decade $^{-1}$) in Alaska, south-eastern Canada and Europe (Fig. 5f). Other regions, such as northern Canada, parts of northern Europe and East Asia showed mixed patterns of SOS trends. One exception is western North America and a few pixels in Quebec and Labrador, where a delay in SOS of more than 1 day per decade was seen (Fig. 5f) – regions where spring temperatures have not increased or

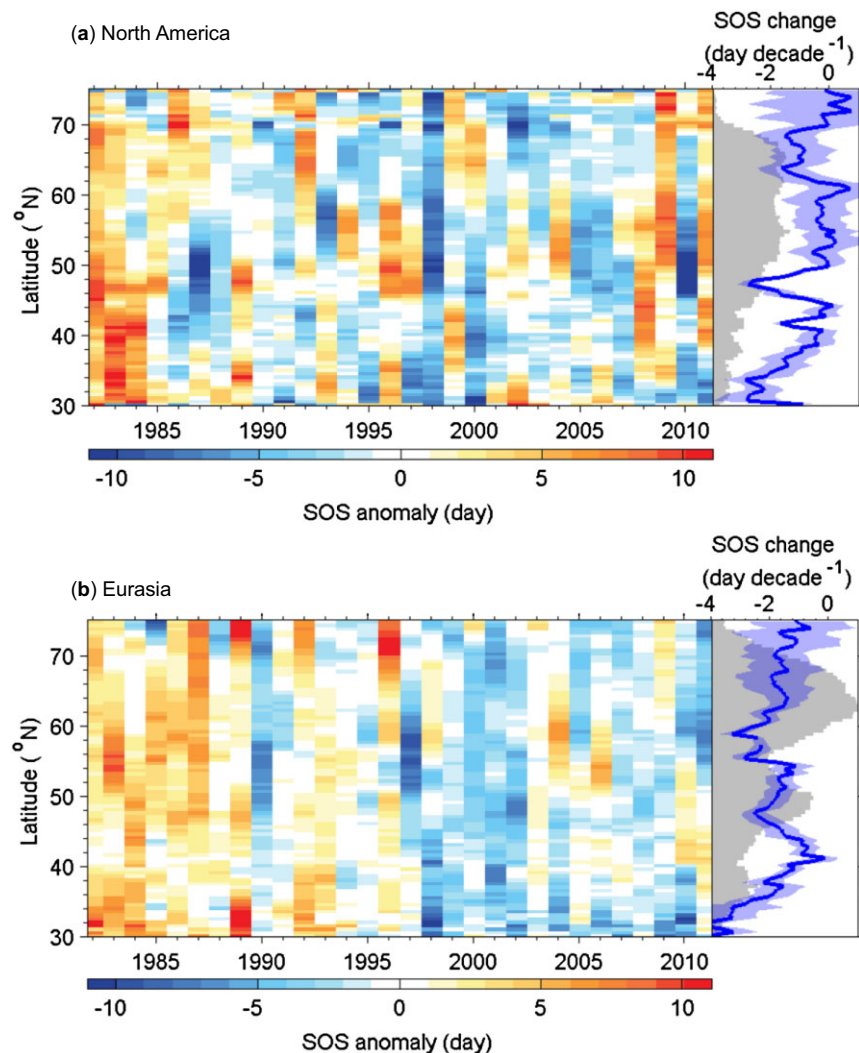


Figure 4 Change in the four-algorithm ensemble mean SOS anomaly for each latitudinal bin (0.5°) from 30° N to 75° N over the period 1982–2011 across (a) North America and (b) Eurasia. The blue curve and blue shaded area in the right-hand panel show the rate of SOS change and its standard deviation for each latitudinal bin, estimated by the linear-model Markov chain Monte Carlo (MCMC). Grey shaded areas show the relative abundance of the vegetated area of each latitudinal bin.

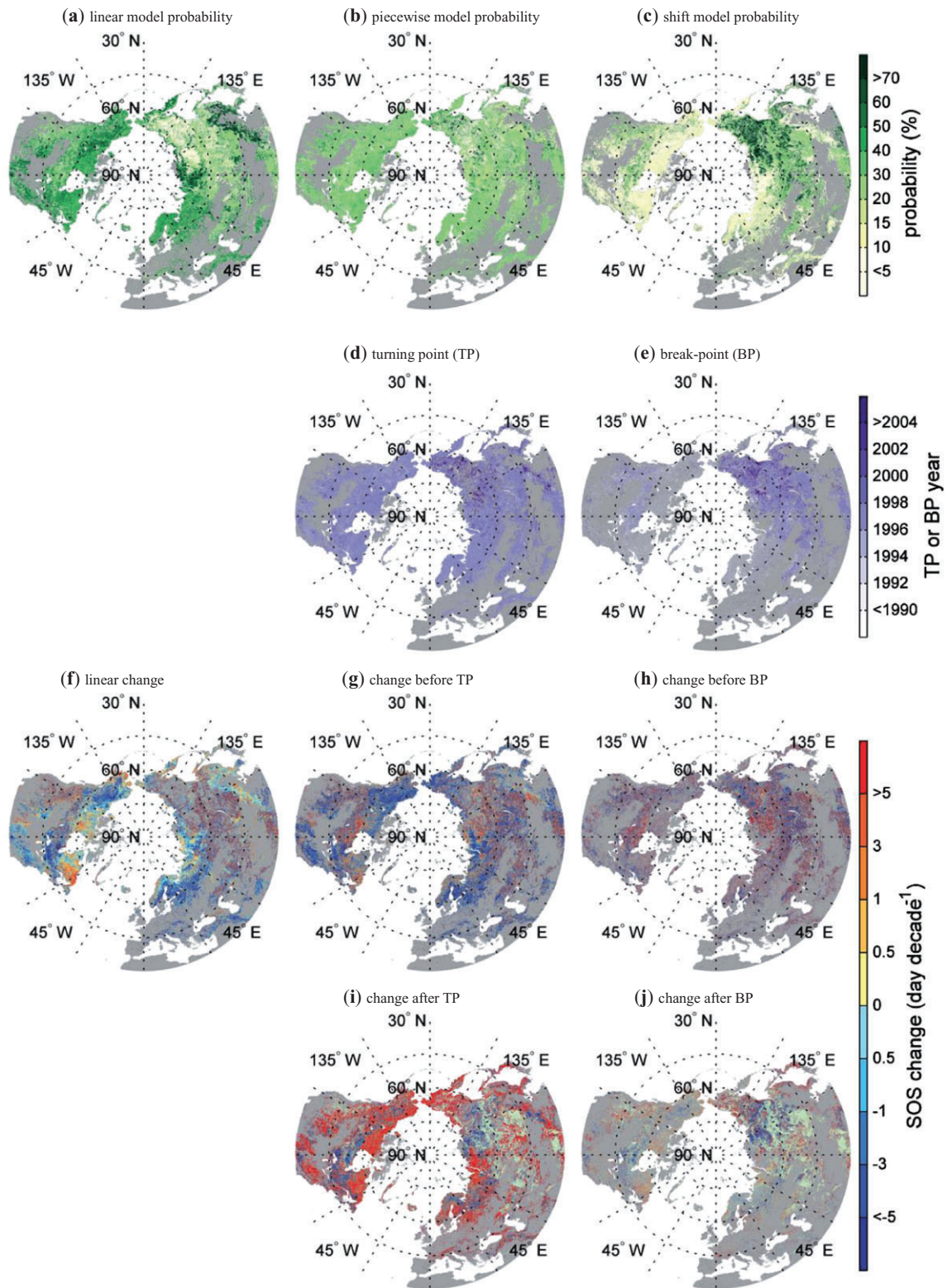


Figure 5 Spatial distribution of the results from reversible-jump Markov chain Monte Carlo (RJ-MCMC). Posterior probability (%) for (a) linear model, (b) piecewise model and (c) shift model; (d) turning point detected by the piecewise model; (e) breakpoint detected by the shift model; (f) start-of-season (SOS) change (days decade⁻¹) estimated by the linear model; (g) SOS change before the turning point estimated by the piecewise model; (h) SOS change before the breakpoint estimated by the shift model; (i) SOS change after the turning point estimated by the piecewise model; (j) SOS change after the breakpoint estimated by the shift model. For panels (d), (g) and (i), only pixels with a posterior probability of the piecewise model higher than 10% are shown. For panels (e), (h) and (j), only pixels with a posterior probability of the shift model higher than 10% are shown.

have even decreased (Fig. S3; Wang *et al.*, 2011; Cohen *et al.*, 2012).

The piecewise model was found to be the most likely model only in a few regions, but even in regions where the linear model was the most likely, the probability of the piecewise model was often not negligible (20–40% over much of the study area) (Fig. 5b). The detected turning points (shown in Fig. 5d for pixels where the probability of the piecewise model is higher than 10%) were mostly found between 1996 and 2000, with 30% of the turning points assigned to 1997. One major exception was eastern Siberia, where turning points occurred after 2000 (Fig. 5d).

The abrupt change (shift) model is very unlikely (< 10%) to have occurred in most regions, but it was the most likely in some central Canadian forests and eastern Siberia (Fig. 5c). Unlike the turning point found by the piecewise model, the breakpoint of abrupt change had considerable spatial inhomogeneity, ranging from the early 1990s to the early 2000s (Fig. 5e). Adjacent areas could show large variation in the breakpoints detected. For example, in eastern Siberia, breakpoints seem to have occurred more widely after 2000, but there are also many pixels in the region with a breakpoint found in the early 1990s (Fig. 5e).

There are few regions, such as Mongolia and the Tibetan Plateau, where the three models were recovered with similar probabilities (Fig. 5a–c). A similarity between the posterior and the prior probability distribution indicates that the SOS derived from satellite data over these regions may not provide sufficient information to separate the posterior probability distribution from the prior, leaving us with little confidence to infer whether there has been any trend change in the SOS in these regions.

SOS change in the most recent decade

Recent studies suggest that NDVI estimates obtained from different satellites could result in different estimates of SOS change (e.g. Zeng *et al.*, 2011). We therefore examined SOS change over the last decade with the NDVI data sets from AVHRR, MODIS and SPOT (Fig. 6a). Variance-decomposition analysis shows that the variation in SOS estimates derived from different satellites was about one-fifth of the variance in estimates derived from different algorithms (Fig. S4). We further examined the SOS change during the estimates' period of common availability (2000–2011) with linear-model MCMC (Fig. 6b). SOS from SPOT showed the largest advance (-5.3 ± 6.4 days decade⁻¹), whereas AVHRR showed a delay (1.0 ± 2.4 days decade⁻¹); SOS derived from MODIS showed an intermediate change (-1.2 ± 10.5 days decade⁻¹). Although the SOS changes derived from SPOT and MODIS data appear to be close to each other, at least of the same sign, the SOS changes estimated from the three data sets were not statistically significant from zero ($P > 0.10$) (Fig. 6b), due to the short time-span, large interannual variations and uncertainties from different SOS extraction algorithms.

DISCUSSION

SOS change over the last three decades

Our estimates of the rate of advance in SOS across the NH over the last 30 years are smaller than previous satellite-based estimates limited to the 1980s and 1990s, which gave rates of advance from -1.9 to -8 days per decade (de Beurs & Henebry, 2005a; Julien & Sobrino, 2009; Jeong *et al.*, 2011). As well as the difference in spatial extent and whether or not uncertainties in SOS extraction are considered, the slower rate of SOS advance over the 30-year period than over the 20-year period might indicate that the SOS advance has slowed down or reversed in the last decade. This conclusion might be supported by analyses of SOS change for the last decade (Fig. 6; Jeong *et al.*, 2011), but trend analyses for short periods are sensitive to natural variability (Easterling & Wehner, 2009), particularly at the beginning and the end of the period analysed (Cong *et al.*, 2013). The large interannual variations of winter and spring climate significantly affect interannual variations in SOS (Maignan *et al.*, 2008). The end of the 1990s and early 2000s

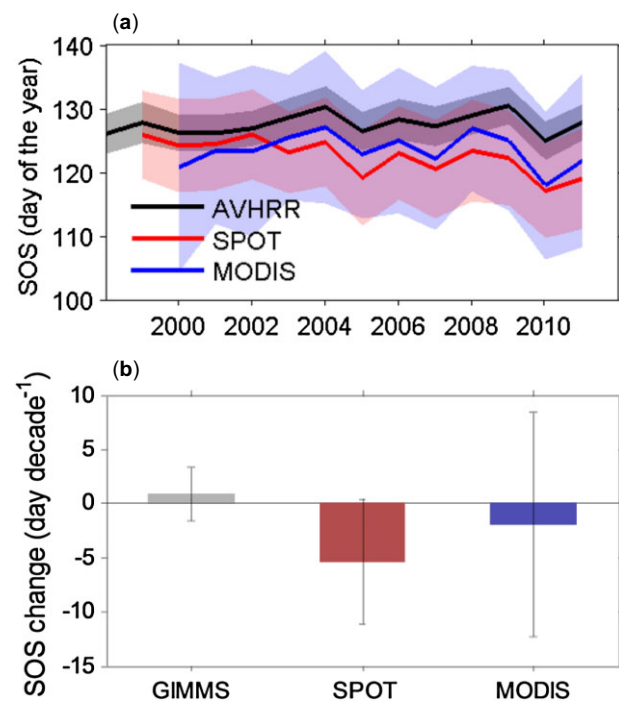


Figure 6 (a) Change in start of season (SOS) over the Northern Hemisphere (NH) during the period 2000–2011 estimated with three NDVI data sets derived from different satellite sensors (AVHRR, Advanced Very High Resolution Radiometer; SPOT, Satellite Pour l'Observation de la Terre; MODIS, Moderate Resolution Imaging Spectroradiometer). (b) Rate of change of SOS over the NH over the period 2000–2011 estimated by linear-model Markov chain Monte Carlo (MCMC). SPOT data were available for 1999–2011, and MODIS data were available during 2000–2011. Solid lines in (a) show the ensemble mean of SOS detected by the four methods, and the shaded area shows the inter-method range of SOS.

saw warm springs that were even warmer than many of the years in the 2000s (Fig. S5). Such climatic events could lead to a few SOS anomalies, resulting in apparent trend changes (larger trend before the event and small or reversed trend afterwards). This signal could also be blurred or amplified by potential errors in SOS algorithms. Thus, a contrasting trend in the last decade is not sufficient evidence for a trend change (Easterling & Wehner, 2009). By considering the interannual variations of the SOS and the uncertainties in SOS extraction, our Bayesian analysis suggests that we have less than 30% confidence that a trend change in SOS has taken place at hemispheric scale (Fig. 3). The 30-year change in SOS over the NH is best described by a linear advance with a trend of -1.4 ± 0.6 days per decade. Interestingly, this rate is well within the range of long-term (longer than 30 years) ground-based phenological studies (e.g. Menzel & Fabian, 1999; Beaubien & Freeland, 2000; Schwartz & Reiter, 2000).

There are large spatial differences in SOS trends between different continents and latitudes. Consistent with the findings of White *et al.* (2009), we found no significant SOS advance over North America, whereas the SOS across Eurasia has advanced significantly over the past three decades (Figs 3 & 4; Barichivich *et al.*, 2013). This is probably associated with less spring warming in North America than in Eurasia (Cohen *et al.*, 2012) because spring phenology is a sensitive biological indicator of climate change (Menzel *et al.*, 2006). The sensitivity of spring phenology to climate change varies, however, between different locations and species (e.g. Maignan *et al.*, 2008). Such differences could be an important driver of the spatial differences in SOS trends. For example, higher latitudes of the NH experienced more dramatic warming than lower latitudes (Hassol, 2004), but the rate of SOS advance at higher latitudes is less than at lower latitudes (Fig. 4). This seems to imply that SOS is less sensitive to warming at higher latitudes than at lower latitudes, a phenomenon which may result from photoperiod limitation (Körner & Basler, 2010) or other climatic factors, such as precipitation or variability in temperature (Peñuelas *et al.*, 2004; Wang *et al.*, 2014).

Despite the linear SOS advance across most of the NH over the last three decades, extrapolating it into proportional SOS advance under future warming would be unwarranted. In parts of eastern and western North America, for instance, the piecewise model has a higher probability than the linear model, with a reversal of the trend occurring in the mid-1990s (Fig. 5). This is consistent with the findings of Pope *et al.* (2013), who observed a reversal of leaf-out date in the mid-1990s in California, although the mechanism for this trend reversal awaits better understanding. It could result either from the stall or reversal of spring temperature (Piao *et al.*, 2011; Wang *et al.*, 2011) or from the lack of winter chilling (endodormancy) under warmer conditions (Yu *et al.*, 2010; Cook *et al.*, 2012; Pope *et al.*, 2013). Our spatial analysis does not appear to support the latter theory, because the reversal of SOS only occurred in a small proportion of the study area that experienced warming over the past three decades. The small proportion of area showing SOS reversal could, however, also be explained by the presence of a minority

of species responding for instance to a lack of winter chilling over temperate ecosystems (Cook *et al.*, 2012), or by the possibility that chilling requirements could have been generally fulfilled under contemporary climate conditions for vegetation north of 40° N (Zhang *et al.*, 2007). If a lack of winter chilling was indeed the primary driver for the changing trend of SOS, slow-downs or reversals of SOS should be expected to become more and more widespread in the future as temperature increases further.

On the other hand, an abrupt change of SOS is also found in a very small fraction of the NH (Fig. 5). Such abrupt changes could be related to large-scale disturbances, such as land-use change, forest-cut or large fires (de Jong *et al.*, 2012). The regions most likely to have experienced abrupt SOS change include parts of central Canada and Siberia, where fire is an important driver of ecosystem dynamics (Sheng *et al.*, 2004; Bond-Lamberty *et al.*, 2007). For example, fires burn around four million hectares of Russian forests per year, and the area burnt is increasing (Hassol, 2004). The impacts of forest and peatland fires on vegetation phenology have attracted much less attention than climatic factors, but fires are able to significantly alter SOS and the regime of SOS change in pre-fire and post-fire periods (Peckham *et al.*, 2008; Risberg & Granström, 2009).

The occurrence of both continuous and abrupt trend changes in a few regions highlight that a non-linear response of SOS to climate change (Cook *et al.*, 2012; Pope *et al.*, 2013) could have taken place over areas such as western and boreal North America and Siberia. With increasing frequency of forest fires expected in the warmer future (Flannigan *et al.*, 2009), fire regime could become an important driver of LSP change over the fire-prone boreal ecosystems. It should be noted that, despite our efforts to consider various uncertainties, it is still imprudent to fully rule out the possibility that some data noise could have contributed to the trend change; detailed regional assessments could thus help for further validation.

Uncertainties in SOS extraction and its implications for trend deduction

Methodological differences have previously been recognized as one of the major reasons for the discrepancies in satellite-derived SOS change detected by different studies (White *et al.*, 2009; Jeong *et al.*, 2011; Cong *et al.*, 2013). These uncertainties are primarily caused by the different filtering functions used to fill data gaps and to minimize the impact of contamination remaining in the NDVI data sets (Cong *et al.*, 2013). For example, larger intermethod differences were found for SOS at higher latitudes (Fig. 2), which might be counterintuitive because higher latitudes usually have a more distinct seasonal cycle. Although the seasonal change in NDVI is larger at higher latitudes, the growing season is shorter, particularly in the Arctic zone, where the growing season can be less than three months. The shorter growing season renders fewer meaningful NDVI observations, given the fixed temporal resolution of NDVI data, and thus fewer constraints on the filter, resulting in larger SOS differences among different methods used.

To the best of our knowledge, this is the first study to explicitly consider the uncertainties in NDVI filtering methods in SOS extraction from satellite data when deducing the historical change of SOS. We argue that the uncertainty in SOS extraction should not be dismissed in such a deduction, because it significantly affects the statistical interpretation. For example, in a statistical experiment, if we reduce the inter-algorithm range of SOS by 30% over NH, the posterior probability of the piecewise model will increase by 8%.

Finally, recent studies have indicated that contemporary Earth system models needed to improve their representation of vegetation phenology (Jeong *et al.*, 2013; Richardson *et al.*, 2013). The rich information provided by the spatiotemporal changes in SOS could, on the one hand, help better understand the mechanisms of how climate change drives SOS. On the other hand, with the explicit representation of uncertainties in the satellite-based observations, we could either confront the models with SOS change or assimilate the SOS change in order to gain confidence in predicting the future evolution of SOS dynamics and its effects on the carbon and hydrological cycles.

ACKNOWLEDGEMENTS

We sincerely acknowledge the contribution of the editors and the two anonymous referees, whose constructive suggestions have significantly improved the manuscript from its earlier version. We thank J. Gash for English revision. This study was supported by the National Natural Science Foundation of China (41125004), National Basic Research Program of China (2013CB956303), National Youth Top-notch Talent Support Program in China and Erasmus Mundus scholarship of the European Union.

REFERENCES

Barichivich, J., Briffa, K.R., Myneni, R.B., Osborn, T.J., Melvin, T.M., Ciais, P., Piao, S.-L. & Tucker, C. (2013) Large-scale variations in the vegetation growing season and annual cycle of atmospheric CO₂ at high northern latitudes from 1950 to 2011. *Global Change Biology*, **19**, 3167–3183.

Beaubien, E.G. & Freeland, H.J. (2000) Spring phenology trends in Alberta, Canada: links to ocean temperature. *International Journal of Biometeorology*, **44**, 53–59.

de Beurs, K.M. & Henebry, G.M. (2004) Land surface phenology, climatic variation, and institutional change: analyzing agricultural land cover change in Kazakhstan. *Remote Sensing of Environment*, **89**, 497–509.

de Beurs, K.M. & Henebry, G.M. (2005a) Land surface phenology and temperature variation in the International Geosphere–Biosphere Program high-latitude transects. *Global Change Biology*, **11**, 779–790.

de Beurs, K.M. & Henebry, G.M. (2005b) A statistical framework for the analysis of long image time series. *International Journal of Remote Sensing*, **26**, 1551–1573.

Bond-Lamberty, B., Peckham, S.D., Ahl, D.E. & Gower, S.T. (2007) Fire as the dominant driver of central Canadian boreal forest carbon balance. *Nature*, **450**, 89–92.

Cleland, E.E., Chuine, I., Menzel, A., Mooney, H.A. & Schwartz, M.D. (2007) Shifting plant phenology in response to global change. *Trends in Ecology and Evolution*, **22**, 357–365.

Cohen, J.L., Furtado, J.C., Barlow, M., Alexeev, V.A. & Cherry, J.E. (2012) Asymmetric seasonal temperature trends. *Geophysical Research Letters*, **39**, L04705.

Cong, N., Wang, T., Nan, H.-J., Ma, Y.-C., Wang, X.-H., Myneni, R.B. & Piao, S.-L. (2013) Changes in satellite-derived spring vegetation green-up date and its linkage to climate in China from 1982 to 2010: a multimethod analysis. *Global Change Biology*, **19**, 881–891.

Cook, B.I., Wolkovich, E.M. & Parmesan, C. (2012) Divergent responses to spring and winter warming drive community level flowering trends. *Proceedings of the National Academy of Sciences USA*, **109**, 9000–9005.

Dee, D.P., Uppala, S.M., Simmons, A.J. *et al.* (2011) The ERA-Interim reanalysis: configuration and performance of the data assimilation system. *Quarterly Journal of the Royal Meteorological Society*, **137**, 553–597.

Easterling, D.R. & Wehner, M.F. (2009) Is the climate warming or cooling? *Geophysical Research Letters*, **36**, L08706.

Flannigan, M., Stocks, B., Turetsky, M. & Wotton, M. (2009) Impacts of climate change on fire activity and fire management in the circumboreal forest. *Global Change Biology*, **15**, 549–560.

Forkel, M., Carvalhais, N., Verbesselt, J., Mahecha, M.D., Neigh, C.S.R. & Reichstein, M. (2013) Trend change detection in NDVI time series: effects of inter-annual variability and methodology. *Remote Sensing*, **5**, 2113–2144.

Hassol, S.J. (2004) *Arctic climate impact assessment: impacts of a warming Arctic*. Cambridge University Press, Cambridge, UK.

Henebry, G.M. & de Beurs, K.M. (2013) Remote sensing of land surface phenology: a prospectus. *Phenology: an integrative science*, 2nd edn (ed. by M. Schwartz), pp. 385–411. Springer, Dordrecht.

Huete, A., Didan, K., Miura, T., Rodriguez, E.P., Gao, X. & Ferreira, L.G. (2002) Overview of the radiometric and biophysical performance of the MODIS vegetation indices. *Remote Sensing of Environment*, **83**, 195–213.

Jeong, S.-J., Ho, C.-H., Gim, H.-J. & Brown, M.E. (2011) Phenology shifts at start vs. end of growing season in temperate vegetation over the Northern Hemisphere for the period 1982–2008. *Global Change Biology*, **17**, 2385–2399.

Jeong, S.-J., Medvigy, D., Shevliakova, E. & Malyshev, S. (2013) Predicting changes in temperate forest budburst using continental-scale observations and models. *Geophysical Research Letters*, **40**, 359–364.

de Jong, R., Verbesselt, J., Schaepman, M.E. & de Bruin, S. (2012) Trend changes in global greening and browning: contribution of short-term trends to longer-term change. *Global Change Biology*, **18**, 642–655.

- Julien, Y. & Sobrino, J.A. (2009) Global land surface phenology trends from GIMMS database. *International Journal of Remote Sensing*, **30**, 3495–3513.
- Kim, Y.-W., Kimball, J.S., Zhang, K. & McDonald, K.C. (2012) Satellite detection of increasing Northern Hemisphere non-frozen seasons from 1979 to 2008: implications for regional vegetation growth. *Remote Sensing of Environment*, **121**, 472–487.
- Körner, C. & Basler, D. (2010) Phenology under global warming. *Science*, **327**, 1461–1462.
- Luysaert, S., Jammot, M., Stoy, P.C. *et al.* (2014) Land management and land-cover change have impacts of similar magnitude on surface temperature. *Nature Climate Change*, **4**, 389–393.
- Maignan, F., Bréon, F.-M., Bacour, C., Demarty, J. & Poirson, A. (2008) Interannual vegetation phenology estimates from global AVHRR measurements: comparison with in situ data and applications. *Remote Sensing of Environment*, **112**, 496–505.
- Maisongrande, P., Duchemin, B. & Dedieu, G. (2004) VEGETATION/SPOT: an operational mission for the Earth monitoring: presentation of new standard products. *International Journal of Remote Sensing*, **25**, 9–14.
- Menzel, A. & Fabian, P. (1999) Growing season extended in Europe. *Nature*, **397**, 659.
- Menzel, A., Sparks, T.H., Estrella, N. *et al.* (2006) European phenological response to climate change matches the warming pattern. *Global Change Biology*, **12**, 1969–1976.
- Peckham, S.D., Ahl, D.E., Serbin, S.P. & Gower, S.T. (2008) Fire-induced changes in green-up and leaf maturity of the Canadian boreal forest. *Remote Sensing of Environment*, **112**, 3594–3603.
- Peñuelas, J., Filella, I., Zhang, X.-Y., Llorens, L., Ogaya, R., Lloret, F., Comas, P., Estiarte, M. & Terradas, J. (2004) Complex spatiotemporal phenological shifts as a response to rainfall changes. *New Phytologist*, **161**, 837–846.
- Peñuelas, J., Rutishauser, T. & Filella, I. (2009) Phenology feedbacks on climate change. *Science*, **324**, 887–888.
- Piao, S.-L., Cui, M.-D., Chen, A.-P., Wang, X.-H., Ciais, P., Liu, J. & Tang, Y.-H. (2011) Altitude and temperature dependence of change in the spring vegetation green-up date from 1982 to 2006 in the Qinghai-Xizang Plateau. *Agricultural and Forest Meteorology*, **151**, 1599–1608.
- Pinzon, J.E. & Tucker, C.J. (2014) A non-stationary 1981–2012 AVHRR NDVI_{3g} time series. *Remote Sensing*, **6**, 6929–6960.
- Pope, K.S., Dose, V., Da Silva, D., Brown, P.H., Leslie, C.A. & DeJong, T.M. (2013) Detecting nonlinear response of spring phenology to climate change by Bayesian analysis. *Global Change Biology*, **19**, 1518–1525.
- Richardson, A.D., Keenan, T.F., Migliavacca, M., Ryu, Y.-R., Sonnentag, O. & Toomey, M. (2013) Climate change, phenology, and phenological control of vegetation feedbacks to the climate system. *Agricultural and Forest Meteorology*, **169**, 156–173.
- Risberg, L. & Granström, A. (2009) The effect of timing of forest fire on phenology and seed production in the fire-dependent herbs *Geranium bohemicum* and *G. lanuginosum* in Sweden. *Forest Ecology and Management*, **257**, 1725–1731.
- Schwartz, M.D. & Reiter, B.E. (2000) Changes in North American spring. *International Journal of Climatology*, **20**, 929–932.
- Sheng, Y.-W., Smith, L.C., MacDonald, G.M., Kremenetski, K.V., Frey, K.E., Velichko, A.A., Lee, M., Beilman, D.W. & Dubinin, P. (2004) A high-resolution GIS-based inventory of the west Siberian peat carbon pool. *Global Biogeochemical Cycles*, **18**, G-3004.
- Stöckli, R. & Vidale, P.L. (2004) European plant phenology and climate as seen in a 20-year AVHRR land-surface parameter data set. *International Journal of Remote Sensing*, **25**, 3303–3330.
- Tucker, C.J., Slayback, D.A., Pinzon, J.E., Los, S.O., Myneni, R.B. & Taylor, M.G. (2001) Higher northern latitude normalized difference vegetation index and growing season trends from 1982 to 1999. *International Journal of Biometeorology*, **45**, 184–190.
- Wang, T., Ottlé, C., Peng, S.-S., Janssens, I.A., Lin, X., Poulter, B., Yue, C. & Ciais, P. (2014) The influence of local spring temperature variance on temperature sensitivity of spring phenology. *Global Change Biology*, **20**, 1473–1480.
- Wang, X.-H., Piao, S.-L., Ciais, P., Li, J.-S., Friedlingstein, P., Koven, C. & Chen, A.-P. (2011) Spring temperature change and its implication in the change of vegetation growth in North America from 1982 to 2006. *Proceedings of the National Academy of Sciences USA*, **108**, 1240–1245.
- White, M.A., de Beurs, K.M., Didan, K. *et al.* (2009) Intercomparison, interpretation, and assessment of spring phenology in North America estimated from remote sensing for 1982–2006. *Global Change Biology*, **15**, 2335–2359.
- Xu, L., Myneni, R.B., Chapin, F.S. *et al.* (2013) Temperature and vegetation seasonality diminishment over northern lands. *Nature Climate Change*, **3**, 581–586.
- Yu, H.-Y., Luedeling, E. & Xu, J.-C. (2010) Winter and spring warming result in delayed spring phenology on the Tibetan Plateau. *Proceedings of the National Academy of Sciences USA*, **107**, 22151–22156.
- Zeng, H.-Q., Jia, G.-S. & Epstein, H. (2011) Recent changes in phenology over the northern high latitudes detected from multi-satellite data. *Environmental Research Letters*, **6**, 045508.
- Zhang, X.-Y., Tarpley, D. & Sullivan, J.T. (2007) Diverse responses of vegetation phenology to a warming climate. *Geophysical Research Letters*, **34**, L19405.

SUPPORTING INFORMATION

Additional supporting information may be found in the online version of this article at the publisher's web-site.

Figure S1 Spatial distribution of the average start of season (SOS) over the period 1982–2011, estimated by four different methods.

Figure S2 Posterior probability (%) of the candidate models for 30-year start-of-season (SOS) change in each 0.5° latitudinal bin from 30° N to 75° N.

Figure S3 Spatial distribution of preseason temperature change over the period 1982–2011.

Figure S4 Inter-satellite and inter-algorithm variance of start of season (SOS) over the period 2000–2011 for three satellites and four algorithms.

Figure S5 Inter-annual variations of preseason temperature change over Eurasia and North America over the period 1982–2011.

BIOSKETCH

Xuhui Wang is a PhD candidate in Peking University, Beijing, China. He has broad research interests particularly in interannual variations and long-term evolutions of vegetation dynamics and carbon cycle of terrestrial ecosystems.

This research was conducted by members of the earth system science research group at Peking University. Members of this group have been dedicated to investigating Northern Hemisphere vegetation changes for more than 10 years. This group also explores the carbon cycle and hydrological cycle of terrestrial ecosystems with various approaches including satellite remote sensing, ecosystem modelling and field experiments.

Editor: Antoine Guisan